

Crosscap Quenches and Entanglement Evolution

Zixia Wei^a and Yasushi Yoneta^b

^a*Jefferson Physical Laboratory, Harvard University, Cambridge, MA 02138, USA*

^b*Center for Quantum Computing, RIKEN, Wako, Saitama 351-0198, Japan*

Abstract

Understanding the mechanisms by which complex correlations emerge through the dynamics of quantum many-body systems remains a fundamental challenge in modern physics. To address this, quench dynamics starting from nonequilibrium states have been extensively studied, leading to significant progress. In this paper, we propose a novel quench protocol, termed the “crosscap quench”, to investigate how highly structured thermal pure states relax into typical ones. We begin by analyzing conformal field theories (CFTs) and derive universal features in the time evolution of entanglement entropy. Furthermore, leveraging the AdS/CFT correspondence, we study holographic CFTs, providing an analytically tractable example in chaotic CFTs. Finally, we validate these findings through numerical simulations in both nonintegrable and integrable quantum spin systems.

Contents

1	Introduction	1
2	Crosscap Quench in CFT and Entanglement Rényi Entropy	3
2.1	Entanglement Structure of Crosscap States	6
2.2	Time Evolution after the Crosscap Quench	8
3	Holographic Crosscap Quench	9
3.1	The Gravity Dual	10
3.2	Holographic Entanglement Entropy and Homology Condition	12
3.3	EE in the Initial State	13
3.4	Time Evolution of EE after the Crosscap Quench	14
4	Crosscap Quench in Nonintegrable Spin Systems	15
5	Crosscap Quench in Integrable Spin Systems	16
6	Conclusion	19

1 Introduction

Understanding the dynamics of quantum many-systems is one of the most important challenges in statistical physics, and quantum quenches [1–3] provide a rich playground for this purpose. A quantum quench is a unitary evolution starting from a pure initial state, triggered by a sudden change of parameters in the system. Through the quench dynamics, we can see how a highly organized initial state evolves into thermal equilibrium in chaotic systems.

In this paper, instead of focusing on the thermalization dynamics, we study a new type of quench where the initial state is already in thermal equilibrium. The initial states we would like to choose are the entangled antipodal pair (EAP) states [4, 5]. Consider a quantum spin-1/2 system on a circle with length $2N$. The EAP state is defined as

$$|\text{EAP}\rangle \equiv \bigotimes_{j=1}^N |\Phi\rangle_{j,j+N}, \quad (1.1)$$

where $|\Phi\rangle_{j,j+N}$ is a maximally entangled state between antipodal pairs of spins at site j and $j + N$. For an arbitrary system, the EAP states are in the microscopic thermal equilibrium (MITE) [6] at infinite temperature, in the sense that they are locally indistinguishable from the canonical Gibbs state with the same temperature, since the reduced density matrix for any geometrically local subsystem A with length smaller than or equal to N is the maximally mixed state. Furthermore, for a 1D Hamiltonian H possessing a certain antiunitary symmetry, such as time-reversal or complex conjugate symmetry, the imaginary-time evolved EAP state

$$|\text{EAP}(\beta)\rangle \equiv \frac{e^{-\frac{\beta}{4}H} |\text{EAP}\rangle}{\sqrt{\langle \text{EAP}|e^{-\frac{\beta}{2}H}|\text{EAP}\rangle}} \quad (1.2)$$

serves as a thermal pure state at inverse temperature β . Thanks to its highly organized entanglement structure, $|\text{EAP}(\beta)\rangle$ can be efficiently prepared using the matrix product states (MPS) [5], despite it exhibits a volume law entanglement.

While $|\text{EAP}(\beta)\rangle$ serves as a thermal pure state, it is a highly atypical one. In fact, it can be easily distinguished from a typical state by the antipodal correlation functions, which are defined on a few degrees of freedom but are considered highly non-local in 1D systems. In this sense, the EAP state utilizes the antipodal entanglement structure to deceive local observers into perceiving thermal equilibrium and at the same time stays easy to simulate.

As a result, even though $|\text{EAP}(\beta)\rangle$ is already in thermal equilibrium, its correlation structure will get more scrambled under chaotic quenches. We will study the time evolution of various type of correlations under such quenches, which will highlight a hierarchy between different notions of thermal equilibrium. We will also study time evolution of EAP states in integrable systems, see how the initial thermal condition deviates from the equilibrium.

Among all the variations, quantum quenches in conformal field theories (CFT) are one of the most well-studied class [3] which is under good analytic control. Therefore, we would like to study quenches from EAP states in both lattice systems and CFTs.

In order to formulate EAP quenches in CFTs, it is useful to note that EAP states in lattice systems are profoundly related to crosscap states in 2D CFT. In 2D CFT, a crosscap state is a state living on the Hilbert space supported on a circle that is realized by performing the Euclidean path integral over a “crosscap”, a spacetime structure obtained by cutting a whole and identifying its antipodal points on a 2D Euclidean manifold. In [7], the authors extend the notions of crosscap states to a class of integrable field theories and a class of

integrable spin chains, where those in integrable spin chains have the same form as the EAP states in Eq. (1.1).

While it stays unclear what the exact relation between crosscap states is in *generic* CFTs and EAP states in spin systems [8], we will compute some universal behavior of the entanglement entropy in CFT crosscap states and argue that they essentially capture the entanglement structure exhibited by the EAP states. Based on this, in the CFT cases, we will study quantum quenches starting from the crosscap states, which we refer to as “crosscap quenches” in this paper.

In section 2, we first formulate the crosscap quench in CFT, and use the replica trick to study some universal behaviors of entanglement Rényi entropy in the initial state to see that it essentially captures the entanglement structure in EAP states. After that, we will use the words “crosscap state (quench)” and “EAP state (quench)” interchangeably. Then we will study some universal behaviors of time evolution of EE after the crosscap quench in CFTs. In section 3, we identify the gravity dual of the crosscap quench in $\text{AdS}_3/\text{CFT}_2$ and study the holographic entanglement entropy. This serves as an analytically tractable example of a crosscap quench in a chaotic CFT. In section 4, we study the crosscap quench in nonintegrable spin systems, and confirm its qualitative consistency with the holographic results. In section 4, we study the crosscap quench in integrable spin systems, and contrast its differences from those in chaotic systems.

Note added: While this paper is under preparation, a very interesting paper [9] came out and also studied time evolution of entanglement entropy from crosscap states but in different systems. The authors of [9] focused on quantum circuit models and integrable fermion chains while we focus on CFT, holography and spin chains in this paper. The integrable fermion chains investigated in [9] should be equivalent to our computations for the transverse-field Ising models in section 5 via the Jordan-Wigner transformation in some regimes.

2 Crosscap Quench in CFT and Entanglement Rényi Entropy

In this section, we first formulate the crosscap quench in CFT and explain how the entanglement Rényi entropy can be computed using the replica trick.

We then study some universal behaviors of the initial state to establish a connection between the crosscap states and the EAP states. After that, we study some universal behaviors appearing in the time evolution.

Let us start by thinking about a Euclidean path integral over a cylinder whose spatial direction is a circle S^1 parameterized by $0 \leq x < 2L$ with $x \sim x + 2L$, and Euclidean time direction is an interval parameterized by $-\alpha \leq \tau \leq 0$. Imposing the boundary condition $|\psi\rangle$ at $\tau = -\alpha$ and $\langle\varphi|$ at $\tau = 0$, the path integral over the cylinder computes $\langle\varphi|e^{-\alpha H}|\psi\rangle$. Therefore, by changing the boundary condition $\langle\varphi|$ at $\tau = 0$, the path integral realizes the wave functional of state $e^{-\alpha H}|\psi\rangle$ at $\tau = 0$.

Now, instead of explicitly imposing a boundary condition $|\psi\rangle$ at $\tau = -\alpha$, we glue it by performing an antipodal identification $x \sim x + L$ at $\tau = -\alpha$. Such a structure is called a crosscap. Due to the crosscap, now the Euclidean path integral only has one boundary at $\tau = 0$ and the topology becomes a Möbius strip. Performing the Euclidean path integral over the crosscap is equivalent to imposing a crosscap state $|C\rangle$ as the “boundary” condition of $\tau = -\alpha$. The crosscap state satisfies the following constraints from consistency condition of 2D CFT [10]

$$(L_n - (-1)^n \bar{L}_{-n}) |C\rangle = 0, \quad (n = 0, 1, 2, \dots), \quad (2.1)$$

where L_n (\bar{L}_n) are holomorphic (anti-holomorphic) Virasoro generators.

As a result, the path integral over such a Möbius strip realizes $e^{-\alpha H}|C\rangle$ on its boundary $\tau = 0$. Accordingly, $\langle C|e^{-\alpha H}$ is realized by its time reflection, and the density matrix $e^{-\alpha H}|C\rangle\langle C|e^{-\alpha H}$ is realized by a combination of them. The inner product $\langle C|e^{-2\alpha H}|C\rangle$ is given by gluing the two boundaries together, and as a result, it is given by a path integral over a tube with two crosscaps on the two ends, which is equivalent to a Klein bottle \mathbb{K}^2 .

$$\langle C|e^{-2\alpha H}|C\rangle = \dots = Z_{\mathbb{K}^2} \quad (2.2)$$

Let us then take the interval $0 \leq x \leq l$ the subsystem A , and use A^C to denote its complement. The (unnormalized) reduced density matrix $\rho_A \equiv \text{Tr}_{A^C} (e^{-\alpha H}|C\rangle\langle C|e^{-\alpha H})$ on A can be realized by gluing the A^C part of the bra Möbius strip and the ket Möbius strip, leaving the boundaries corresponding to A open.

Based on this, we can apply the replica method developed in [11] to compute the entanglement Rényi entropy of subsystem A . We can realize ρ_A^n by preparing n copies of ρ_A , and then gluing the upper half of the slit in the i -th copy to the lower half in the i -th copy, and $\text{Tr}(\rho_A^n)$ by gluing the two remaining two boundaries in ρ_A . This is a path integral over a n -replicated manifold Σ_n with $2n$ crosscaps.

$$\text{Tr}(\rho_A^n) = Z_{\Sigma_n}. \quad (2.3)$$

With this notation, $\Sigma_1 = \mathbb{K}^2$. As a result, the entanglement Rényi entropy can be computed as

$$S_A^{(n)} = \frac{1}{1-n} \log \frac{\text{Tr}(\rho_A^n)}{(\text{Tr}\rho_A)^n} = \frac{1}{1-n} \log \frac{Z_{\Sigma_n}}{(Z_{\Sigma_1})^n}. \quad (2.4)$$

The explicit evaluation of this expression requires computing the partition function on the replicated manifold Σ_n , which is often complicated. Instead of thinking of Z_{Σ_n} as the partition function of n manifolds, it turns out to be useful to regard it alternatively as a n -replicated theory on the original manifold Σ_1 , with one twist operator σ_n inserted at $(\tau, x) = (0, 0)$, and another twist operator $\tilde{\sigma}_n$ inserted at $(\tau, x) = (0, l)$ [12]. Given a local operator $O^{(i)}$ in the i -th copy of the theory and moving it around σ_n ($\tilde{\sigma}_n$) with angle 2π , it turns into the corresponding local operator $O^{(i+1)}$ ($O^{(i-1)}$) in the $(i+1)$ -th ($(i-1)$ -th) copy of the theory. The twist operators behave as primary operators with chiral and anti-chiral conformal dimension

$$h_n = \bar{h}_n = \frac{c}{24} \left(n - \frac{1}{n} \right). \quad (2.5)$$

In this description, the entanglement Rényi entropy can be computed with the correlation function of the twist operators on the Klein bottle [12],

$$S_A^{(n)} = \frac{1}{1-n} \log \langle \sigma(0, 0) \tilde{\sigma}(0, l) \rangle_{\mathbb{K}^2}, \quad (2.6)$$

where the correlation function is computed in the replicated theory. In general, if the subsystem A is taken as a multi-interval between (τ_{a_i}, x_{a_i}) and (τ_{b_i}, x_{b_i}) , the corresponding entanglement Rényi entropy can be computed with

$$S_A^{(n)} = \frac{1}{1-n} \log \left\langle \prod_i \sigma(\tau_{a_i}, x_{a_i}) \tilde{\sigma}(\tau_{b_i}, x_{b_i}) \right\rangle_{\mathbb{K}^2}. \quad (2.7)$$

The von Neumann entropy, or entanglement entropy, can be obtained by taking the $n \rightarrow 1$ limit of the Rényi entropy

$$S_A = \lim_{n \rightarrow 1} S_A^{(n)}. \quad (2.8)$$

To evaluate the correlation function of twist operators on the Klein bottle, it is useful to apply the doubling trick. The Klein bottle parameterized by $\tau \in [-\alpha, \alpha]$ and $x \in [0, 2L]$ admits a torus \mathbb{T}^2 parameterized by $\tau \in [-2\alpha, 2\alpha]$ and $x \in [0, 2L]$ as a double cover. The Klein bottle is obtained from the torus by performing the \mathbb{Z}_2 quotient $(\tau, x) \sim (2\alpha - \tau, x + L)$.

Accordingly, inserting a twist operator $\sigma(\tau, x)$ on \mathbb{K}^2 corresponds to simultaneously inserting $\sigma(\tau, x)$ and $\tilde{\sigma}(2\alpha - \tau, x + L)$ on \mathbb{T}^2 . More precisely,

$$\begin{aligned} & \left\langle \prod_i \sigma(\tau_{a_i}, x_{a_i}) \tilde{\sigma}(\tau_{b_i}, x_{b_i}) \right\rangle_{\mathbb{K}^2} \\ &= \sqrt{\left\langle \prod_i \sigma(\tau_{a_i}, x_{a_i}) \tilde{\sigma}(\tau_{b_i}, x_{b_i}) \prod_j \tilde{\sigma}(2\alpha - \tau_{a_j}, x_{a_j} + L) \sigma(2\alpha - \tau_{b_j}, x_{b_j} + L) \right\rangle_{\mathbb{T}^2}}. \end{aligned} \quad (2.9)$$

Note that the mirror image of σ turns out to be $\tilde{\sigma}$.

In the following, we study some universal behaviors of entanglement Rényi entropy in regularized crosscap states $e^{-\alpha H}|C\rangle$ and its time evolution in the quench dynamics. The strategy is to focus on situations where the correlation function can be reduced to the OPE limits of pairs of σ and $\tilde{\sigma}$, such that the vacuum blocks dominate the computations. We will not consider the OPE limits between σ and σ or those between $\tilde{\sigma}$ and $\tilde{\sigma}$, since the identity primary does not appear in these limits due to the conservation of the twist number. We will leave the study of these OPE limits as future works.

2.1 Entanglement Structure of Crosscap States

Following the strategy sketched above, let us study the entanglement structure of the regularized crosscap state $e^{-\alpha H}|C\rangle$, and see how it resembles that of the EAP states (1.2).

For the analysis below, it is useful to note that the two-point function of a scalar operator O with $h_O = \bar{h}_O$ on an infinite cylinder parameterized by $x \in (-\infty, \infty)$ and $\tau \in [-2\alpha, 2\alpha]$ is

$$\langle O(\tau_1, x_1) O(\tau_2, x_2) \rangle_{\text{cylinder}} = \left(\frac{\pi}{2\alpha} \right)^{4h_O} \left[2 \cosh \left(\frac{\pi(x_1 - x_2)}{2\alpha} \right) - 2 \cos \left(\frac{\pi(\tau_1 - \tau_2)}{2\alpha} \right) \right]^{-2h_O}. \quad (2.10)$$

Single interval

The first situation we would like to consider is a single interval subsystem A given by $0 \leq x \leq l$. At the thermodynamic limit limit $\alpha/L \ll 1$, in the regime $l/L \ll 1$,

$$\langle \sigma(0, 0) \tilde{\sigma}(0, l) \rangle_{\mathbb{K}^2} = \sqrt{\langle \sigma(0, 0) \tilde{\sigma}(0, l) \sigma(2\alpha, l + \pi) \tilde{\sigma}(2\alpha, \pi) \rangle_{\mathbb{T}^2}} \quad (2.11)$$

$$\approx \sqrt{\langle \sigma(0, 0) \tilde{\sigma}(0, l) \rangle_{\text{cylinder}} \langle \sigma(2\alpha, l + \pi) \tilde{\sigma}(2\alpha, \pi) \rangle_{\text{cylinder}}} \quad (2.12)$$

$$= \left(\frac{\pi}{2\alpha} \right)^{4h_n} \left[2 \cosh \left(\frac{\pi l}{2\alpha} \right) - 2 \right]^{-2h_n} = \left(\frac{\pi}{4\alpha} \right)^{4h_n} \left[\sinh \left(\frac{\pi l}{4\alpha} \right) \right]^{-4h_n} \quad (2.13)$$

Accordingly,

$$S_A^{(n)} = \frac{c}{6} \left(1 + \frac{1}{n} \right) \log \left[\frac{4\alpha}{\pi\epsilon} \sinh \left(\frac{\pi l}{4\alpha} \right) \right], \quad (\alpha/L \ll 1, \ l/L \ll 1), \quad (2.14)$$

where ϵ is a UV cutoff corresponding to the lattice distance. When $l/\alpha \gg 1$,

$$S_A^{(n)} = \frac{\pi cl}{24\alpha} \left(1 + \frac{1}{n} \right) + \dots, \quad (\alpha/L \ll 1, \ l/L \ll 1, \ \alpha/l \ll 1), \quad (2.15)$$

and exhibits the volume law entanglement.

This is nothing but the thermal spectrum for a system at inverse temperature $\beta = 4\alpha$. Therefore, a regularized crosscap state with cutoff α exhibits the same entanglement spectrum for single interval subsystems as the EAP state (1.2) at inverse temperature $\beta = 4\alpha$, at the thermodynamic limit.

Similarly, the entanglement entropy for a large subsystem has entanglement Rényi entropy

$$S_A^{(n)} = \frac{c}{6} \left(1 + \frac{1}{n} \right) \log \left[\frac{4\alpha}{\pi\epsilon} \sinh \left(\frac{\pi(2L-l)}{4\alpha} \right) \right], \quad (\alpha/L \ll 1, \ (L-l)/L \ll 1), \quad (2.16)$$

manifesting the pure state nature of $e^{-\alpha H} |C\rangle$.

Antipodal double intervals

The next example we would like to consider is the double interval subsystem $0 \leq x \leq l$ and $L \leq x \leq L + l$, where the two components are located antipodally. We again take the thermodynamic limit $\alpha/L \ll 1$. In the regime $\alpha/l \ll 1$, the 4-point function

$$\begin{aligned} & \langle \sigma(0,0) \tilde{\sigma}(0,l) \sigma(0,\pi) \tilde{\sigma}(0,\pi+l) \rangle_{\mathbb{K}^2} \\ &= \sqrt{\langle \sigma(0,0) \tilde{\sigma}(0,l) \sigma(0,\pi) \tilde{\sigma}(0,\pi+l) \tilde{\sigma}(2\alpha,0) \sigma(2\alpha,l) \tilde{\sigma}(2\alpha,\pi) \sigma(2\alpha,\pi+l) \rangle_{\mathbb{T}^2}} \\ & \approx \langle \sigma(0,0) \tilde{\sigma}(2\alpha,0) \rangle_{\text{cylinder}}^2 = \left(\frac{\pi}{4\alpha} \right)^{8h_n}. \end{aligned} \quad (2.17)$$

Accordingly,

$$S_A^{(n)} = \frac{c}{3} \left(1 + \frac{1}{n} \right) \log \left[\frac{4\alpha}{\pi\epsilon} \right], \quad (\alpha/L \ll 1, \ \alpha/l \ll 1), \quad (2.18)$$

which exhibits an area law entanglement. In particular, if we consider the high temperature limit and take $\alpha/\epsilon = O(1)$, then the antipodal double interval A has almost no entanglement with its complement. This again matches the entanglement structure of antipodally located subsystems in EAP states.

Based on the universal behavior of the entanglement Rényi entropy studied above, we can say that crosscap states serve as the analogue of EAP states in generic CFTs. This contrasts the conformal boundary states satisfying

$$(L_n - \bar{L}_{-n}) |B\rangle = 0, \quad (2.19)$$

which essentially does not contain spatial entanglement at the leading order [13].

2.2 Time Evolution after the Crosscap Quench

Let us then study the time evolution of the entanglement entropy. To this end, we compute the correlation function of twist operators for general insertion points $w = x + i\tau$, and then perform the analytic continuation $\tau \rightarrow it$. Some universal behaviors are investigated below.

Single Interval

For a single interval subsystem A given by $0 \leq x \leq l$. At the thermodynamic limit $\alpha/L \ll 1$, in the regime $l/L \ll 1$ and $t/L \ll 1$,

$$\begin{aligned} \langle \sigma(\tau, 0) \tilde{\sigma}(\tau, l) \rangle_{\mathbb{K}^2} \Big|_{\tau \rightarrow it} &= \sqrt{\langle \sigma(\tau, 0) \tilde{\sigma}(\tau, l) \sigma(2\alpha - \tau, l + \pi) \tilde{\sigma}(2\alpha - \tau, \pi) \rangle_{\mathbb{T}^2}} \Big|_{\tau \rightarrow it} \\ &= \sqrt{\langle \sigma(0, -t) \tilde{\sigma}(0, l - t) \sigma(2\alpha, l + \pi + t) \tilde{\sigma}(2\alpha, \pi + t) \rangle_{\mathbb{T}^2}} \\ &\approx \sqrt{\langle \sigma(0, -t) \tilde{\sigma}(0, l - t) \rangle_{\text{cylinder}} \langle \sigma(2\alpha, l + \pi + t) \tilde{\sigma}(2\alpha, \pi + t) \rangle_{\text{cylinder}}} \\ &= \left(\frac{\pi}{4\alpha}\right)^{4h_n} \left[\sinh\left(\frac{\pi l}{4\alpha}\right) \right]^{-4h_n} \end{aligned} \quad (2.20)$$

Therefore,

$$S_A^{(n)} = \frac{c}{6} \left(1 + \frac{1}{n}\right) \log \left[\frac{4\alpha}{\pi\epsilon} \sinh\left(\frac{\pi l}{4\alpha}\right) \right], \quad (\alpha/L \ll 1, \ l/L \ll 1, \ t/L \ll 1), \quad (2.21)$$

From this, we can see that, at the thermodynamic limit, the entanglement spectrum for a finite-size single interval does not change within finite time in the crosscap quench dynamics.

Antipodal double interval

For the double interval subsystem $0 \leq x \leq l$ and $L \leq x \leq L + l$ located antipodally, in a similar manner, at $\alpha/L \ll 1, \alpha/l \ll 1, t/l \ll 1$,

$$\begin{aligned} & \langle \sigma(\tau, 0) \tilde{\sigma}(\tau, l) \sigma(\tau, \pi) \tilde{\sigma}(\tau, \pi + l) \rangle_{\mathbb{K}^2} |_{\tau \rightarrow it} \\ &= \sqrt{\langle \sigma(0, -t) \tilde{\sigma}(0, l - t) \sigma(0, \pi - t) \tilde{\sigma}(0, \pi + l - t) \tilde{\sigma}(2\alpha, t) \sigma(2\alpha, l + t) \tilde{\sigma}(2\alpha, \pi + t) \sigma(2\alpha, \pi + l + t) \rangle_{\mathbb{T}^2}} \\ & \approx \langle \sigma(0, -t) \tilde{\sigma}(2\alpha, t) \rangle_{\text{cylinder}}^2 = \left(\frac{\pi}{4\alpha} \right)^{8h_n} \cosh \left(\frac{\pi t}{2\alpha} \right)^{-8h_n} \end{aligned} \quad (2.22)$$

The entanglement Rényi entropy then turns out to be

$$S_A^{(n)} = \frac{c}{3} \left(1 + \frac{1}{n} \right) \log \left[\frac{4\alpha}{\pi\epsilon} \cosh \left(\frac{\pi t}{2\alpha} \right) \right], \quad (\alpha/L \ll 1, \alpha/l \ll 1, t/l \ll 1), \quad (2.23)$$

which exhibits a linear growth at late time

$$S_A^{(n)} = \frac{\pi ct}{6\alpha} \left(1 + \frac{1}{n} \right) + \dots, \quad (\alpha/L \ll 1, l/L \ll 1, t/l \ll 1, \alpha/t \ll 1). \quad (2.24)$$

If we instead focus on double interval systems with $l/L \ll 1$, and look at the behavior at very late time $l/t \ll 1$ (but suppressed at the thermodynamic limit $t/L \ll 1$), then

$$S_A^{(n)} = \frac{c}{3} \left(1 + \frac{1}{n} \right) \log \left[\frac{4\alpha}{\pi\epsilon} \sinh \left(\frac{\pi l}{4\alpha} \right) \right], \quad (\alpha/L \ll 1, l/L \ll 1, l/t \ll 1, t/L \ll 1). \quad (2.25)$$

By comparing these expressions with that at the initial state (2.18), we can see that, under the crosscap quench, such a antipodal double interval subsystem initially exhibits the area law entanglement, then experiences a linear growth of entanglement, and eventually converges to the volume law thermal spectrum. This dynamics shows how the initial crosscap state, which is already in thermal equilibrium but engineered with highly organized entanglement structure, relaxes into a more scrambled few-body thermalization under the time evolution.

3 Holographic Crosscap Quench

In the previous section, we formulated the crosscap quench in CFT and studied some universal behaviors of the entanglement Rényi entropy.

In this section, we study the crosscap quench in the AdS/CFT correspondence [14–16] and apply the Ryu-Takayanagi (RT) formula [17, 18] and its covariant version, the Hubeny-Rangamani-Takayanagi (HRT) formula [19], to study the entanglement entropy in the holographic crosscap quench dynamics, assuming their validity. This serves as an explicit example of a chaotic critical system, where the entanglement entropy can be explicitly computed.

As we have already seen in the previous section, the crosscap quench is described by the unitary time evolution starting from a regularized crosscap state

$$e^{-itH} e^{-\alpha H} |C\rangle, \quad (3.1)$$

which is prepared by a Schwinger-Keldysh path integral from a Klein bottle. The gravity dual of such a CFT has been worked out in [14] and turned out to be the so-called \mathbb{RP}^2 geon geometry in AdS_3 [20]. Besides, the holographic entanglement entropy associated with the geon geometry has been investigated in [21]. Therefore, the computations presented in this section are not new, but are to be reinterpreted as the crosscap quench in holography and compared with results in other sections.

In the following, we first present the AdS dual of such a crosscap quench, and then compute the holographic entanglement entropy. To match the standard convention used in the gravity side, we set

$$\alpha = \frac{\beta}{4}, \quad 2L = 2\pi, \quad (3.2)$$

throughout this section.

3.1 The Gravity Dual

In the $\text{AdS}_3/\text{CFT}_2$ correspondence, when the boundary geometry is a Klein bottle \mathbb{K}^2 with a sufficiently high temperature (i.e. sufficiently small β), the bulk dual is given by the Euclidean geon geometry [14, 22–24]. The metric is identical to that of a BTZ black hole:

$$ds^2 = (r^2 - r_H^2) d\tau^2 + \frac{dr^2}{r^2 - r_H^2} + r^2 dx^2, \quad (3.3)$$

where $r = r_H \equiv 2\pi/\beta$ is the location of the event horizon. The difference from the BTZ black hole, however, is a \mathbb{Z}_2 quotient:

$$(\tau, x, r) \sim \left(\frac{\beta}{2} - \tau, x + \pi, r \right). \quad (3.4)$$

Let us firstly focus on the geometry of the $\tau = 0$ time slice. While the $r > r_H$ part of the geometry is identical to that of the BTZ black hole, a crosscap is inserted at the horizon $r = r_H$. As the result, the topology of the $\tau = 0$ slice is the Möbius strip. This is the gravity dual of $e^{-\frac{\beta}{4}H} |C\rangle$, the initial state of the crosscap quench.

Performing the analytic continuation $\tau = it$, the metric turns out to be

$$ds^2 = - (r^2 - r_H^2) dt^2 + \frac{dr^2}{r^2 - r_H^2} + r^2 dx^2. \quad (3.5)$$

To describe the interior of the black hole, let us extend the coordinate to the Kruskal coordinate with

$$\tilde{U} \equiv \pm \sqrt{\frac{r - r_H}{r + r_H}} e^{r_H t_{\mp}}, \quad (3.6)$$

$$\tilde{V} \equiv \mp \sqrt{\frac{r - r_H}{r + r_H}} e^{-r_H t_{\mp}}, \quad (3.7)$$

where t_- is the time t obtained by $\tau = it_-$, and t_+ is the time direction on the other side of the black hole obtained by $\tau = \beta/2 - it_+$. With the Kruskal coordinate, the metric then turns out to be

$$ds^2 = \frac{-4 d\tilde{U} d\tilde{V} + (-1 + \tilde{U}\tilde{V})^2 r_H^2 dx^2}{(1 + \tilde{U}\tilde{V})^2}. \quad (3.8)$$

We can also introduce a time-like coordinate \tilde{T} and a space-like coordinate \tilde{X} with

$$\tilde{U} \equiv \tilde{T} - \tilde{X}, \quad (3.9)$$

$$\tilde{V} \equiv \tilde{T} + \tilde{X}, \quad (3.10)$$

with which the metric is now

$$ds^2 = \frac{-4 d\tilde{T}^2 + 4 d\tilde{X}^2 + (-1 + \tilde{T}^2 - \tilde{X}^2)^2 r_H^2 dx^2}{(1 + \tilde{T}^2 - \tilde{X}^2)^2}. \quad (3.11)$$

The \mathbb{Z}^2 quotient is

$$(\tilde{T}, x, \tilde{X}) \sim (\tilde{T}, x + \pi, -\tilde{X}). \quad (3.12)$$

This one-sided black hole is the gravity dual of the crosscap quench dynamics $e^{-itH} e^{-\frac{\beta}{4}H} |C\rangle$. The topology of each Cauchy slice is the Möbius strip and hence non-orientable. However, this non-orientability cannot be verified by an asymptotic observer. This is because that the crosscap sits at $\tilde{X} = 0$, which is behind the event horizon and hence can never be probed by any communication with an asymptotic observer.

3.2 Holographic Entanglement Entropy and Homology Condition

In the following, we apply the Ryu-Takayanagi (RT) formula [17, 18] and the Hubeny-Rangamani-Takayanagi (HRT) formula [19] to compute the entanglement entropy in the crosscap quench dynamics.

In $\text{AdS}_{d+1}/\text{CFT}_d$, a time slice of the CFT describe a quantum state of a $(d-1)$ -dimensional quantum system. Taking a time slice and then divide the spatial region of the CFT into A and B . S_A , the entanglement entropy of the subsystem A , can be computed using its AdS dual with the HRT formula. The procedure is as follows. The subregion A is $(d-1)$ -dimensional and hence codimension-2 from the AdS point of view. We are going to look for a spacelike codimension-2 surface γ_A , which shares the boundary with the subregion A , i.e. $\partial\gamma_A = \partial A$, satisfies the homology constraint,

$$\gamma_A \sim A \iff \exists \text{ spacelike codimension-1 } \mathcal{R}_A \text{ surface s.t. } \partial\mathcal{R}_A = \gamma_A \cup A, \quad (3.13)$$

and is extremal under small perturbations. Among all such codimension-2 surface γ_A , the one with the minimal area (called the HRT surface) is related to the entanglement entropy of subsystem A as,

$$S_A = \min_{\substack{\partial\gamma_A = \partial A \\ \gamma_A \sim A}} \text{ext} \frac{\text{Area}(\gamma_A)}{4G_N^{(d+1)}}, \quad (3.14)$$

where $G_N^{(d+1)}$ is the Newton constant of the bulk AdS. In the following, we will denote the HRT surface as Γ_A to make a distinction with other candidates. The HRT formula is applicable in setups with general time dependence. In special cases when the whole setup is static or when the time slice we are focusing on posits a time reflection symmetry, the HRT formula reduces to the RT formula, where one first restricts to the time-reflection symmetric Cauchy slice, and then look for the minimal surface in it.

In the following, we would like to compute the entanglement entropy of the crosscap quench in holography. Since we are interested in the time evolution, we need to apply the HRT formula. However, the $\tau = 0$ slice is symmetric under the time-reflection, so the RT formula is applicable.

Moreover, each Cauchy slice of the bulk dual of the crosscap quench includes a crosscap in it, and is hence non-orientable. Therefore, the homology constraint (3.13) will turn out to be crucial in the holographic analysis.

We will firstly focus on the $t = 0$ time slice, where the RT formula is applicable to illustrate the nontrivialness of the homology condition, and then compute the time evolution of the entanglement entropy.

3.3 EE in the Initial State

Let us firstly apply the RT formula to study the entanglement entropy associated to the initial state at $t = 0$. In this process, the treatment of the homology condition will become clear.

The whole system

The simplest choice of subsystem A is the entire system. In this case, the state ρ_A is a pure state and hence the entanglement entropy must be zero. Let us confirm this results is reproduced by the RT formula. The topology of the $t = 0$ time slice is a Möbius strip. It is simple but essential to note that the empty set \emptyset satisfies the homology constraint (3.13) by identifying the whole $t = 0$ time slice as \mathcal{R}_A . Therefore, the holographic EE computed by the RT formula is indeed zero.

Single Interval

Let us then take the subsystem A to be a single interval $0 \leq x \leq l$. In this case, there are two types of geodesics γ_A such that $\partial\gamma_A = \partial A$ and satisfy the homology constraint $\gamma_A \sim A$. In the first case, the geodesic γ_A can be obtained by continuously deforming A , and the corresponding \mathcal{R}_A does not contain a crosscap. In the second case, the geodesic γ_A cannot be obtained by continuously deforming A , and the corresponding \mathcal{R}_A contains the crosscap. There also exist geodesics that do not satisfy the homology constraint. This happens when the geodesic γ_A “goes through” the crosscap, and cannot be obtained from A by a continuous deformation. As a result, there are two competing candidates of the RT surfaces, and the EE turns out to be

$$S_A = \min \left\{ \frac{c}{3} \log \left[\frac{\beta}{\pi\epsilon} \sinh \left(\frac{\pi l}{\beta} \right) \right], \frac{c}{3} \log \left[\frac{\beta}{\pi\epsilon} \sinh \left(\frac{\pi(2\pi-l)}{\beta} \right) \right] \right\}. \quad (3.15)$$

Here, we have used the Brown-Henneaux relation $1/4G_N = c/6$ [25]. We can also check that this result matches the universal behavior (2.14) and (2.16) computed in the previous section.

Antipodal double interval

The last example we would like to consider is the antipodally located double interval $0 \leq x \leq l$ and $\pi \leq x \leq \pi + l$. In this case, there are three candidates of RT surfaces satisfying the homology constraint. Compared to the single interval case, the RT surface now can “go across” the crosscap. As a result, the EE turns out to be a competition between the three candidates.

$$S_A = \min \begin{cases} \frac{2c}{3} \log \left[\frac{\beta}{\pi\epsilon} \sinh \left(\frac{\pi l}{\beta} \right) \right] \\ \frac{2c}{3} \log \left[\frac{\beta}{\pi\epsilon} \right] \\ \frac{2c}{3} \log \left[\frac{\beta}{\pi\epsilon} \sinh \left(\frac{\pi(2\pi-l)}{\beta} \right) \right]. \end{cases} \quad (3.16)$$

This is again consistent with the useful behavior (2.18) investigated on the CFT side. We can see that the EE firstly grow, and then saturate, and then decrease. In other words, the crosscap state exhibits an area law for antipodally located double interval. This is natural since the crosscap state $|C\rangle$ defined on S^1 can be regarded as a product state defined on S^1/Z_2 where the Z_2 is the antipodal identification map. It is known that the Euclidean time evolution of a product state in 1D quantum many-body system generically exhibits an EE scales as $O(cl^0 \log \beta)$ [26].

3.4 Time Evolution of EE after the Crosscap Quench

Then we would like to compute the holographic EE under the time evolution. Similar to the reasoning in the $t = 0$ case, the HRT surface for the entire system is the empty set $\Gamma_A = \emptyset$ and its EE stays to be zero. This manifests the unitarity of the time evolution.

For the single interval, there are again two candidates of the RT surfaces. Both of them stay outside the event horizon and their lengths do not change in time. As a result, the EE for a single interval stays to be (3.15).

For the antipodal double intervals, on the other hand, the RT surface goes across the crosscap travels inside the event horizon and exhibits a nontrivial time evolution, while the two other candidate RTs stays to be invariant under the time evolution. As a result, we have

$$S_A = \min \begin{cases} \frac{2c}{3} \log \left[\frac{\beta}{\pi\epsilon} \sinh \left(\frac{\pi l}{\beta} \right) \right] \\ \frac{2c}{3} \log \left[\frac{\beta}{\pi\epsilon} \cosh \left(\frac{2\pi t}{\beta} \right) \right] \\ \frac{2c}{3} \log \left[\frac{\beta}{\pi\epsilon} \sinh \left(\frac{\pi(2\pi-l)}{\beta} \right) \right]. \end{cases} \quad (3.17)$$

We can see that the EE exhibits a linear growth at late time, and eventually saturates to a volume law entanglement. These are also consistent with the universal behavior in CFT investigated in section 2.2.

4 Crosscap Quench in Nonintegrable Spin Systems

Returning to the lattice theory, we numerically compute the time evolution of entanglement under dynamics starting from an EAP state and compare the results with the field-theoretic predictions discussed in the previous sections.

We begin our numerical analysis with the case where the Hamiltonian is nonintegrable. Here, we consider the spin-1/2 Heisenberg chain with next-nearest-neighbor interactions, defined by the Hamiltonian

$$H = \sum_{j=1}^N \sigma_j^x \sigma_{j+1}^x + \sigma_j^y \sigma_{j+1}^y + \sigma_j^z \sigma_{j+1}^z + J \sum_{j=1}^N \sigma_j^x \sigma_{j+2}^x + \sigma_j^y \sigma_{j+2}^y + \sigma_j^z \sigma_{j+2}^z. \quad (4.1)$$

It was shown that this model is nonintegrable [27, 28]. We set the coupling J at the quantum critical point $J = 0.241167$, which is well described by a CFT with central charge $c = 1$ [29–31].

As an initial state, we choose the EAP state $|\text{EAP}\rangle$ defined by Eq. (1.1) with $|\Phi\rangle_{j,j+N} \propto |0\rangle_j |0\rangle_{j+N} + |1\rangle_j |1\rangle_{j+N}$

$$|\text{EAP}\rangle = \bigotimes_{j=1}^N \frac{|0\rangle_j |0\rangle_{j+N} + |1\rangle_j |1\rangle_{j+N}}{\sqrt{2}}. \quad (4.2)$$

Here, $|0\rangle_j$ and $|1\rangle_j$ are the eigenvectors of σ_j^z in the local Hilbert space associated with site j . Consequently, the state at time t is given by

$$|\text{EAP}(t)\rangle = e^{-iHt} |\text{EAP}\rangle. \quad (4.3)$$

We numerically calculate the entanglement entropy S_A of this state for various choices of subsystems A .

Figure 1 shows the dynamics of entanglement entropy for the single interval $A = \{1, 2, \dots, l\}$ and the antipodally located double interval $A = \{1, 2, \dots, l/2\} \cup \{N+1, N+2, \dots, N+l/2\}$. For $l \gg L$, the entanglement entropy exhibits an initial linear growth and saturates at a

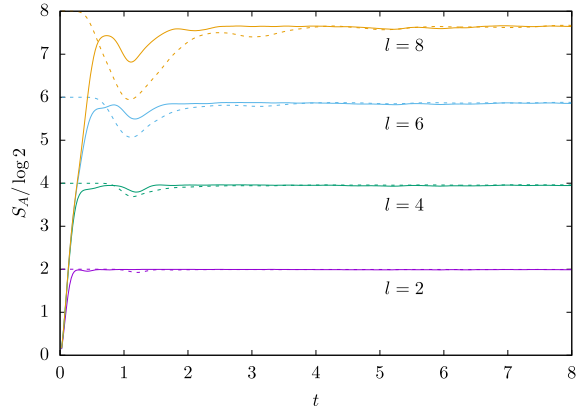


Figure 1: Entanglement entropy S_A of the time-evolved EAP state $|\text{EAP}(t)\rangle$ in the critical Heisenberg chain with next-nearest-neighbor interactions as a function of t for total system size $2N = 20$ and various subsystem size l , with solid lines representing the antipodally located double intervals $A = \{1, 2, \dots, l/2\} \cup \{N + 1, N + 2, \dots, N + l/2\}$ and dashed lines represent the single intervals $A = \{1, 2, \dots, l\}$.

constant value, in well agreement with CFT predictions. Moreover, this saturated value coincides with the thermodynamic entropy at $\beta = 0$. These results implies that the EAP state acquires a complex correlation structure and relaxes into a few-body thermal state.

As illustrated in Fig. 2a, the time-evolved EAP state $|\text{EAP}(t)\rangle$ contains a volume-law entanglement, with a slight deviation increasing as the subsystem size grows, and the deviation becomes most pronounced when the subsystem size is exactly half of the total system size. Furthermore, we plot the system-size dependence of the deviation in Fig. 2b. It can be seen that the deviation is subextensive. This is consistent with the results obtained from the analysis of holographic CFTs. Furthermore, we find that the deviation scales as $N^{1/2}$ in the thermodynamic limit.

5 Crosscap Quench in Integrable Spin Systems

In this section, for comparison with the nonintegrable case analyzed in the previous section, we examine the entanglement dynamics of the EAP state in an integrable critical quantum spin chain. Specifically, we consider the transverse-field Ising chain, which is integrable and

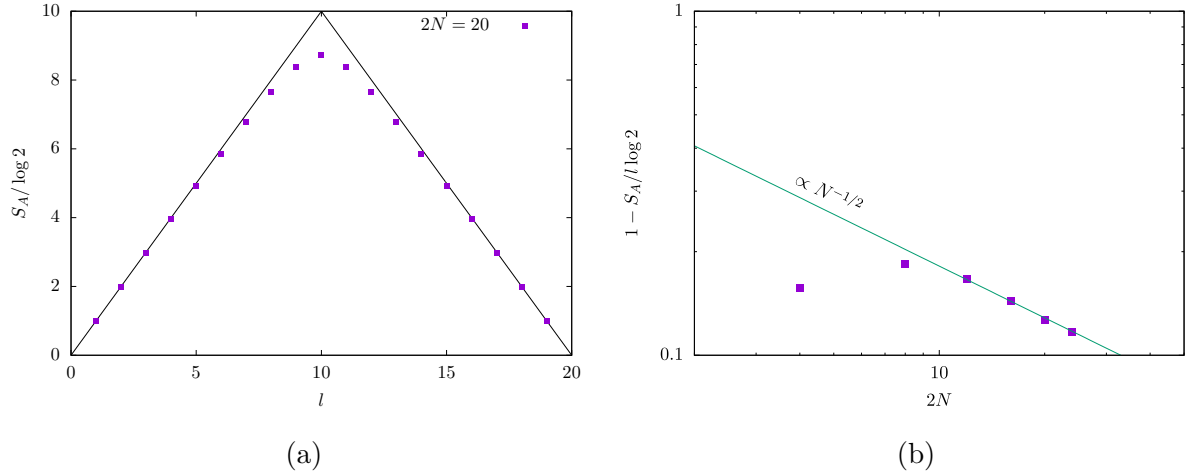


Figure 2: (a) Time-averaged entanglement entropy of the time-evolved EAP state $|\text{EAP}(t)\rangle$ in the critical Heisenberg chain with next-nearest-neighbor interactions, averaged over the time interval $t \in [8, 16]$, as a function of the subsystem size l for the single interval A in a system of size $2N = 20$. The solid line represents the entanglement of the initial EAP state, which is maximally entangled for any single interval. (b) Deviation from the maximum value at $l = N$. The solid line serves as a guide to the eye and is proportional to $N^{-1/2}$.

exhibits quantum criticality, defined by the Hamiltonian

$$H = - \sum_{j=1}^N \sigma_j^z \sigma_{j+1}^z - g \sum_{j=1}^N \sigma_j^x. \quad (5.1)$$

The quantum critical point is located at $g = 1$ and is well described by CFT with central charge $c = 1/2$ [11, 32]. As in the previous section, we consider the dynamics starting from the EAP state (4.2) defined with $|\Phi\rangle_{j,j+N} \propto |0\rangle_j |0\rangle_{j+N} + |1\rangle_j |1\rangle_{j+N}$.

In Fig. 3, we show the dynamics of the entanglement entropy for the single interval $A = \{1, 2, \dots, l\}$ and the antipodally located double interval $A = \{1, 2, \dots, l/2\} \cup \{N+1, N+2, \dots, N+l/2\}$. For $l \ll L$, similar to the nonintegrable case, the entanglement entropy exhibits an initial linear growth followed by saturation at the thermodynamic entropy for $\beta = 0$. This reflects the universality of the result obtained from the CFT analysis in Section 2, which is independent of the details of the theory, such as the integrability. Consequently, even in the integrable systems, the EAP state relaxes into a few-body thermal state.

In contrast, when the subsystem size l becomes comparable to the total system size, $l \sim N$, the situation differs. It can be seen that for large subsystems, the entanglement

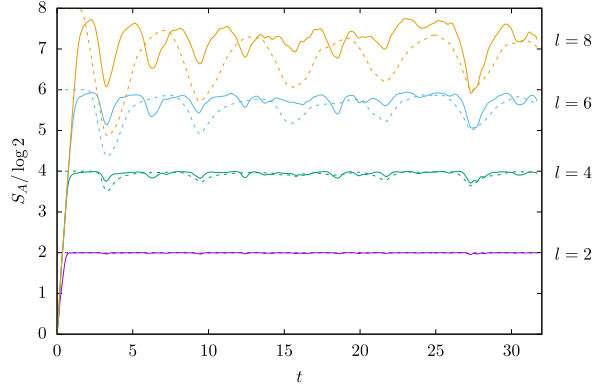


Figure 3: Entanglement entropy S_A of the time-evolved EAP state $|\text{EAP}(t)\rangle$ in the critical transverse-field Ising chain as a function of t for total system size $2N = 24$ and various subsystem size l , with solid lines representing the antipodally located double intervals $A = \{1, 2, \dots, l/2\} \cup \{N + 1, N + 2, \dots, N + l/2\}$ and dashed lines represent the single intervals $A = \{1, 2, \dots, l\}$.

entropy does not equilibrate but instead oscillates. Furthermore, as shown in Figs. 4a and 4b, the deviation from the maximum entanglement of the single interval initially contained in the EAP state, caused by time evolution, is extensive, unlike in nonintegrable systems.

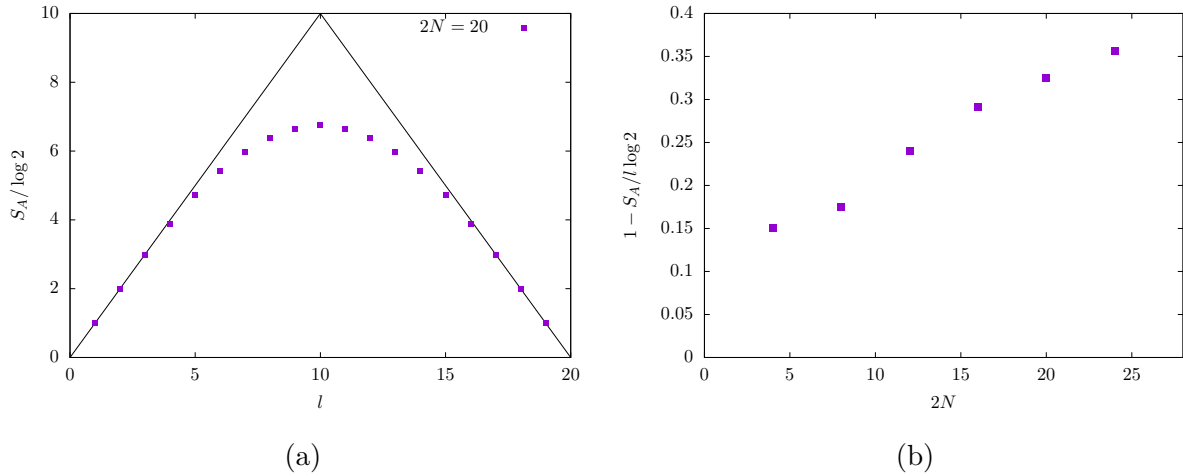


Figure 4: (a) Time-averaged entanglement entropy of the time-evolved EAP state $|\text{EAP}(t)\rangle$ in the critical transverse-field Ising chain, averaged over the time interval $t \in [8, 32]$, as a function of the subsystem size l for the single interval A in a system of size $2N = 20$. The solid line represents the entanglement of the initial EAP state, which is maximally entangled for any single interval. (b) Deviation from the maximum value at $l = N$.

Therefore, while the EAP state in an integrable system also relaxes into a few-body thermal state, the resulting state exhibits an entanglement structure that is qualitatively distinct from that of the nonintegrable cases.

6 Conclusion

In this paper, we have studied quantum quenches in 1D many-body systems starting from crosscap states and EAP states. While EAP states are originally defined in spin systems, we have argued that crosscap states serve as good analogues of them in CFT because they exhibit similar entanglement structures. This was demonstrated by studying the universal behavior of the entanglement Rényi entropy of CFT crosscap states. Based on this, we termed the quenches starting from crosscap states and EAP states as "crosscap quenches." We then investigated the time evolution of entanglement in both general CFT and holographic settings of crosscap quenches, with the latter serving as an analytically tractable example of chaotic systems. Additionally, we numerically studied crosscap quenches in both a non-integrable critical spin chain and an integrable critical spin chain.

In the non-integrable systems studied in this paper, local subsystems, such as small single intervals, exhibit a volume law for entanglement and are expected to remain thermal throughout the dynamics. On the other hand, the entanglement entropy of antipodally located double intervals initially exhibits an area law, followed by linear growth, and eventually saturates to a volume law. This behavior illustrates how the initially well-organized thermal state becomes scrambled under time evolution and transitions into a state of few-body thermalization. Conversely, the integrable system deviates from the initially well-organized thermal equilibrium and exhibits oscillations in the time evolution of entanglement.

Acknowledgements

We are grateful to Yuya Kusuki, Diandian Wang and Zhencheng Wang for useful discussions and comments. ZW is supported by the Society of Fellows at Harvard University. YY is supported by the Special Postdoctoral Researchers Program at RIKEN.

References

- [1] P. Calabrese and J. L. Cardy, *Evolution of entanglement entropy in one-dimensional systems*, *J. Stat. Mech.* **0504** (2005) P04010 [[cond-mat/0503393](#)].
- [2] P. Calabrese and J. L. Cardy, *Time-dependence of correlation functions following a quantum quench*, *Phys. Rev. Lett.* **96** (2006) 136801 [[cond-mat/0601225](#)].
- [3] P. Calabrese and J. Cardy, *Quantum quenches in 1 + 1 dimensional conformal field theories*, *J. Stat. Mech.* **1606** (2016) 064003 [[1603.02889](#)].
- [4] Y. Chiba and Y. Yoneta, *Exact Thermal Eigenstates of Nonintegrable Spin Chains at Infinite Temperature*, *Phys. Rev. Lett.* **133** (2024) 170404 [[2403.12330](#)].
- [5] Y. Yoneta, *Thermal pure states for systems with antiunitary symmetries and their tensor network representations*, *Phys. Rev. Res.* **6** (2024) L042062 [[2407.14454](#)].
- [6] T. Mori, T. Ikeda, E. Kaminishi and M. Ueda, *Thermalization and prethermalization in isolated quantum systems: a theoretical overview*, *J. Phys. B* **51** (2018) 112001 [[1712.08790](#)].
- [7] J. Caetano and S. Komatsu, *Crosscap States in Integrable Field Theories and Spin Chains*, *J. Stat. Phys.* **187** (2022) 30 [[2111.09901](#)].
- [8] B.-Y. Tan, Y. Zhang, H.-C. Zhang, W. Tang, L. Wang, H.-H. Tu et al., *Extracting the Luttinger parameter from a single wave function*, [2402.18364](#).
- [9] K. Chalas, P. Calabrese and C. Rylands, *Quench dynamics of entanglement from crosscap states*, [2412.04187](#).
- [10] N. Ishibashi, *The Boundary and Crosscap States in Conformal Field Theories*, *Mod. Phys. Lett. A* **4** (1989) 251.
- [11] P. Calabrese and J. Cardy, *Entanglement entropy and quantum field theory*, *J. Stat. Mech.* **2004** (2004) P06002.
- [12] J. L. Cardy, O. A. Castro-Alvaredo and B. Doyon, *Form factors of branch-point twist fields in quantum integrable models and entanglement entropy*, *J. Stat. Phys.* **130** (2007) 129–168 [[0706.3384](#)].

- [13] M. Miyaji, S. Ryu, T. Takayanagi and X. Wen, *Boundary States as Holographic Duals of Trivial Spacetimes*, *JHEP* **05** (2015) 152 [[1412.6226](#)].
- [14] J. M. Maldacena, *Eternal black holes in anti-de Sitter*, *JHEP* **04** (2003) 021 [[hep-th/0106112](#)].
- [15] S. S. Gubser, I. R. Klebanov and A. M. Polyakov, *Gauge theory correlators from noncritical string theory*, *Phys. Lett.* **B428** (1998) 105 [[hep-th/9802109](#)].
- [16] E. Witten, *Anti-de Sitter space and holography*, *Adv. Theor. Math. Phys.* **2** (1998) 253 [[hep-th/9802150](#)].
- [17] S. Ryu and T. Takayanagi, *Holographic derivation of entanglement entropy from AdS/CFT*, *Phys. Rev. Lett.* **96** (2006) 181602 [[hep-th/0603001](#)].
- [18] S. Ryu and T. Takayanagi, *Aspects of Holographic Entanglement Entropy*, *JHEP* **08** (2006) 045 [[hep-th/0605073](#)].
- [19] V. E. Hubeny, M. Rangamani and T. Takayanagi, *A Covariant holographic entanglement entropy proposal*, *JHEP* **07** (2007) 062 [[0705.0016](#)].
- [20] J. Louko and D. Marolf, *Single exterior black holes and the AdS / CFT conjecture*, *Phys. Rev. D* **59** (1999) 066002 [[hep-th/9808081](#)].
- [21] H. Maxfield, *Entanglement entropy in three dimensional gravity*, *JHEP* **04** (2015) 031 [[1412.0687](#)].
- [22] M. Guica and S. F. Ross, *Behind the geon horizon*, *Class. Quant. Grav.* **32** (2015) 055014 [[1412.1084](#)].
- [23] A. Maloney and S. F. Ross, *Holography on Non-Orientable Surfaces*, *Class. Quant. Grav.* **33** (2016) 185006 [[1603.04426](#)].
- [24] Z. Wei, *Holographic Dual of Crosscap Conformal Field Theory*, [2405.03755](#).
- [25] J. D. Brown and M. Henneaux, *Central Charges in the Canonical Realization of Asymptotic Symmetries: An Example from Three-Dimensional Gravity*, *Commun. Math. Phys.* **104** (1986) 207.

- [26] Y. Kusuki, K. Tamaoka, Z. Wei and Y. Yoneta, *Efficient simulation of low-temperature physics in one-dimensional gapless systems*, *Phys. Rev. B* **110** (2024) L041122 [[2309.02519](#)].
- [27] N. Shiraishi, *Absence of Local Conserved Quantity in the Heisenberg Model with Next-Nearest-Neighbor Interaction*, *J. Stat. Phys.* **191** (2024) 114 [[2403.04522](#)].
- [28] T. C. Hsu and J. C. Angles d'Auriac, *Level repulsion in integrable and almost-integrable quantum spin models*, *Phys. Rev. B* **47** (1993) 14291.
- [29] K. Okamoto and K. Nomura, *Fluid-dimer critical point in $S = 1/2$ antiferromagnetic Heisenberg chain with next nearest neighbor interactions*, *Phys. Lett. A* **169** (1992) 433.
- [30] K. Nomura and K. Okamoto, *Critical properties of $S = 1/2$ antiferromagnetic XXZ chain with next-nearest-neighbour interactions*, *J. Phys. A. Math. Gen.* **27** (1994) 5773.
- [31] S. Eggert, *Numerical evidence for multiplicative logarithmic corrections from marginal operators*, *Phys. Rev. B* **54** (1996) R9612 [[9602026](#)].
- [32] S. Sachdev, *Quantum Phase Transitions*. Cambridge University Press, Cambridge, England, 2011.